nature materials

ARTICLES

PUBLISHED ONLINE: 12 SEPTEMBER 2010 | DOI: 10.1038/NMAT2834

Highly sensitive flexible pressure sensors with microstructured rubber dielectric layers

Stefan C. B. Mannsfeld[1], Benjamin C-K. Tee[2], Randall M. Stoltenberg[3], Christopher V. H-H. Chen[1], Soumendra Barman[1], Beinn V. O. Muir[1], Anatoliy N. Sokolov[1], Colin Reese[1] and Zhenan Bao[1]*

The development of an electronic skin is critical to the realization of artificial intelligence that comes into direct contact with humans, and to biomedical applications such as prosthetic skin. To mimic the tactile sensing properties of natural skin, large arrays of pixel pressure sensors on a flexible and stretchable substrate are required. We demonstrate flexible, capacitive pressure sensors with unprecedented sensitivity and very short response times that can be inexpensively fabricated over large areas by microstructuring of thin films of the biocompatible elastomer polydimethylsiloxane. The pressure sensitivity of the microstructured films far surpassed that exhibited by unstructured elastomeric films of similar thickness, and is tunable by using different microstructures. The microstructured films were integrated into organic field-effect transistors as the dielectric layer, forming a new type of active sensor device with similarly excellent sensitivity and response times.

To produce electronic skin that emulates the properties of natural skin, large arrays of pressure-sensitive pixels on a flexible and stretchable substrate are required. Promising routes towards stretchable matrix-type substrates[1] and stretchable electrodes[2–4] have been demonstrated in the past. However, there is still a need for a low-cost and large-area-compatible technology for producing pressure-sensitive pixels with sufficient sensitivity in both medium- (10–100 kPa, suitable for object manipulation) and low-pressure regimes (<10 kPa, comparable to gentle touch[5]).

Organic field-effect transistors (OFETs) have been successfully used as active elements in display panels and sensor devices[6], and are considered key elements in large-area fabrication of logic elements on plastic and flexible substrates. Recently, OFETs were demonstrated to operate stably even under water[7]. The OFET architecture is, therefore, an ideal choice for the active pixel element in a pressure-sensor array on flexible substrates for potential application as electronic skin. OFET technology has been used as the readout element for conductive rubber pressure sensors in pioneering works[1,8], but neither pressure sensitivity in the low-pressure regime nor sufficient sensor responsiveness have been reported.

We present a new type of organic thin-film pressure-sensing device structure, in which one of the key layers in the OFET structure—the dielectric—consists of a thin, regularly structured rubber that is compressible and makes the devices highly pressure sensitive. The direct dependence of the output current on the dielectric capacitance in OFET devices enables the sensing of an applied pressure. This device design, including the structured-rubber dielectric concept, provides substantially higher sensitivity in both medium- and low-pressure regimes than in previous reports, and the devices exhibit unprecedentedly fast response and relaxation times ($\ll$1 s).

Interesting demonstrations have been made incorporating static pressure sensing into conventional silicon metal–oxide–semiconductor field-effect transistor (MOSFET) technology[9,10]. However, the so-called PRESSFET technology, based on rigid Si substrates, is difficult to implement on flexible substrates, relies on high-cost Si manufacturing processes, and provides substantially lower pressure sensitivity than that achieved in this work. Moreover, it cannot reliably sense low pressure values (<10 kPa) owing to its very large thermal signal shift of $\sim$4 kPa K^{-1}. So far, only a few types of pressure sensor on flexible substrates have been reported. The pressure-dependent resistance of a sensitized rubber thin film was used in a variety of sensor devices[1,8,11,12], but was insensitive in the low-pressure regime (<1 g mm^{-2}, $<\sim$10 kPa) and susceptible to significant hysteresis[11]. Sensors in which external loads were detected as capacitance changes of air gaps[13,14] also exhibited poor or no sensitivity in the low-pressure regime. Capacitive sensors employing a polymer foam were demonstrated, but are $\sim$1,000 times less pressure sensitive and exhibit response/relaxation times that are 10–100 times slower than those attained in this work[15]. Pressure sensors have been made using a piezoelectric elastomer[16,17], but are not suitable for integration into flexible electronic skin[16], and are 10–30 times less pressure sensitive than our devices. A pressure sensor based on a similar ferroelectric polymer composite only senses pressures greater than 1 MPa (ref. 18). Capacitive coupling of polymer ferroelectret actuators to the gate electrodes of OFETs on flexible substrates[19] is a promising route, but they are currently sensitive to static pressure loads $\geq$ 2 kPa (herein as low as 3 Pa) with about half the sensitivity achieved here, and are far more complex to fabricate[19]. Also, the low degree of uniformity of the cellular ferroelectret foam on the micrometre scale may limit the down-scaling of this technology to a higher sensor-matrix resolution. OFETs without any compressible element show extremely low pressure sensitivity[20], long relaxation times[20,21] and a poorly understood sensing mechanism.

The key component of our material design is the microstructuring of thin films of the dielectric elastomer polydimethylsiloxane (PDMS). PDMS is well known for its good elastic properties, its biomedical compliance with human tissue[22] and living cells[23], and its high performance as a dielectric material in OFETs (refs 24, 25). These attributes make PDMS the material of choice for

[1]Department of Chemical Engineering, Stanford University, Stanford, California 94305, USA, [2]Department of Electrical Engineering, Stanford University, Stanford, California 94305, USA, [3]Department of Chemistry, Stanford University, Stanford, California 94305, USA. *e-mail: zbao@stanford.edu.

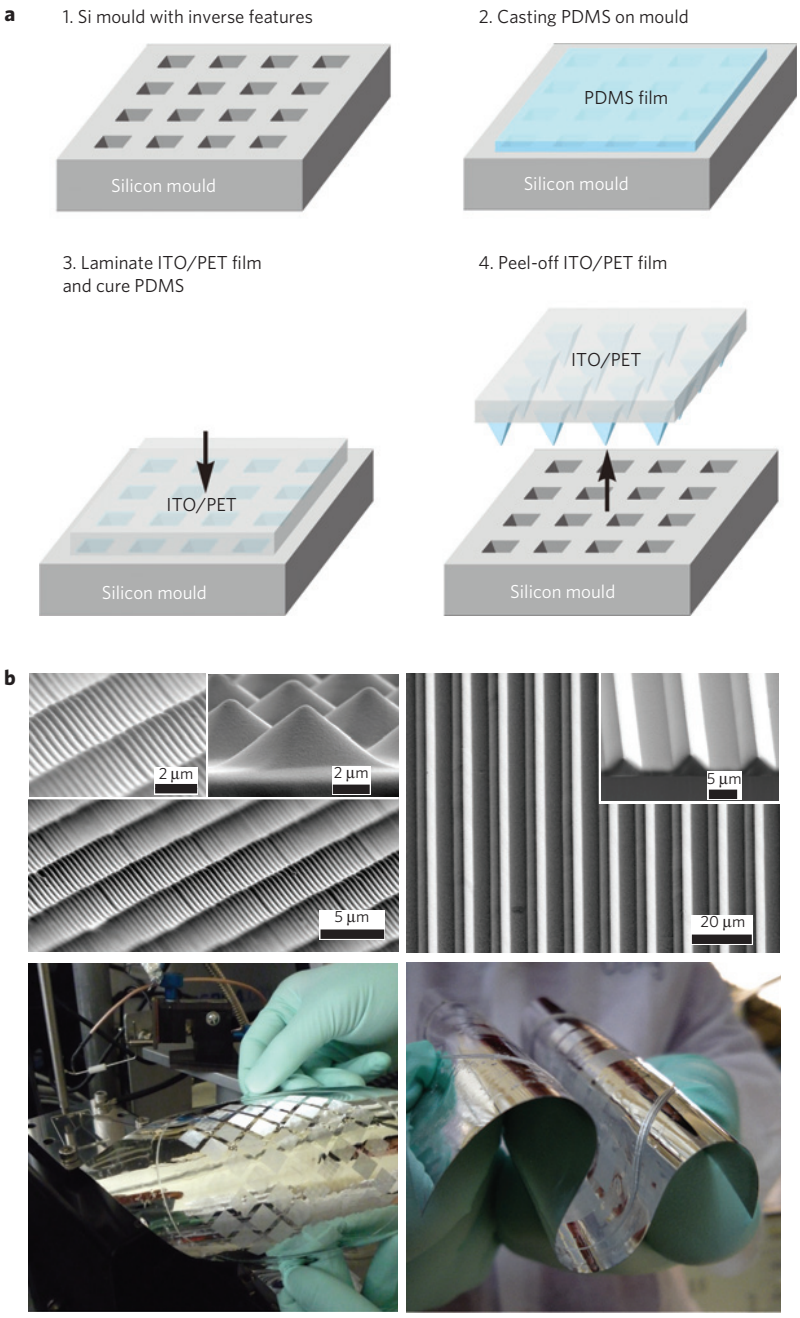

Figure 1 | Fabrication of microstructured PDMS films. a, Schematic process for the fabrication of microstructured PDMS films. A dilute solution of the PDMS mixture of base and cross-linker in hexane is drop cast onto a Si wafer mould (Step 1) containing arrays of the inverse of the features to be replicated (Step 2). The PDMS film is vacuum-degassed and partially cured. An ITO-coated PET substrate is laminated to the mould, and the PDMS film is cured under pressure at a temperature of 70 °C for about three hours (Step 3). Application of even pressure during the curing is crucial to obtain arrays of PDMS features with uniform size across the entire substrate. After curing, the flexible substrate is peeled off the mould (Step 4). **b**, Top, SEM images of the microstructured PDMS films. Two-dimensional arrays of square pyramids are formed from arrays of pyramidal recesses etched into the face of a (100)-cut Si-wafer mould (left). Line features can also be produced and show the same uniformity and regularity across centimetre length scales as is observed with the pyramidal feature arrays (right). Bottom, The pressure-sensitive structured PDMS films can be moulded at full-wafer scale (100 mm) with high uniformity and fidelity on a variety of flexible, plastic substrates (shown here is aluminium-coated PET film).

pressure-sensitive dielectric thin films, especially with regard to integration with artificial skin. However, although thicker solid PDMS films (millimetre to several hundred micrometres) are nearly fully elastic in the <100 kPa pressure regime, thin films of only a few micrometres in thickness are subject to significant visco-elastic creep. This results in increased relaxation times after compression due to irreversible entanglement of polymer chains and the lack of deformable surfaces, that is, inability to displace material in response to a load. Microstructuring the PDMS thin films provides voids that enable the microstructure surfaces to elastically deform on application of external pressure, thereby storing and releasing the energy reversibly, and thus minimizing the problems associated with visco-elastic behaviour.

The microstructured surface was fabricated by moulding a surface topology into the PDMS films before cross-linking, as shown in Fig. 1a. The microstructures in the PDMS film are regular

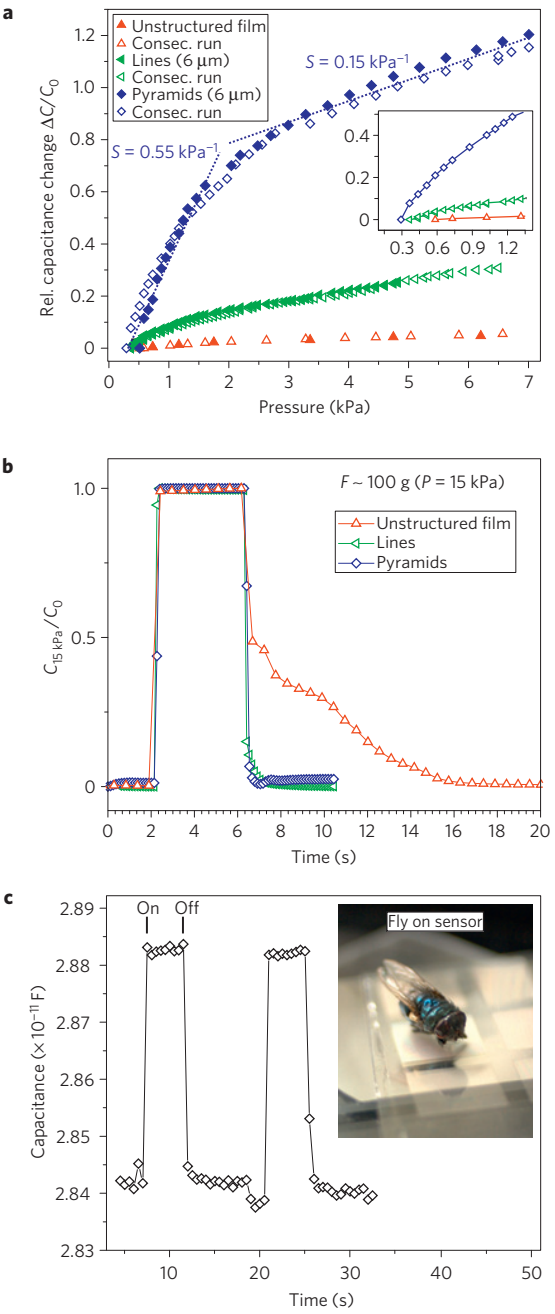

Figure 2 | Characterization of the capacitive pressure response of microstructured PDMS films. a, Pressure-response curves for different types of microstructured PDMS films of feature size 6 μm (both size and pitch). The structured PDMS films exhibit a much higher pressure sensitivity than the unstructured PDMS films of the same thickness. The maximum slope of the relative capacitance change of the pyramidal film in the 0.2 kPa range is 0.55 kPa^{-1}. This is about 30 times higher than the sensitivity of the unstructured film in the same range. **b**, Relaxation and steady-state curves for different types of feature after loading (15 kPa for 4 s) and unloading. Both structured and unstructured PDMS films show immediate response to the application of pressure. However, the structured PDMS films exhibit relaxation times in the millisecond range on complete release of the pressure, whereas the unstructured films return to the original unloaded state capacitance after more than 10 s. **c**, The microstructured PDMS films are able to sense the application of very small pressures. Shown is the capacitance change on placing and removing a bluebottle fly (20 mg) on an area of 64 mm^2, corresponding to a pressure of only 3 Pa.

and uniform (2–3% pitch fidelity) across the full size of the wafer mould, as can be seen from the highly parallel rows of identically high pyramids in scanning electron microscope (SEM) images (top of Fig. 1b and insets). Features are replicated with high quality even on very thin (<100 μm) and highly flexible plastic sheets (bottom of Fig. 1b). This is important for the large-area compatibility of a pressure sensor with a capacitive sensing scheme, because the tallest three PDMS features will always determine the contact plane for the counter-electrode; thus a small variance in the height of the features ensures a clearly defined and reproducible top contact plane.

The pressure sensitivity of the microstructured PDMS films was tested in thin-film capacitors that were completed by laminating an indium tin oxide (ITO)-coated conductive flexible poly(ethyleneterephthalate) (PET) sheet on top of the PDMS film surface. Here we limit the discussion to 6-μm-sized PDMS features. Smaller features down to 3 μm were also produced with excellent and consistent quality, as well as reproducible pressure sensitivity. Even greater sensitivity was obtained with features smaller than 3 μm, but they were more susceptible to defects as a result of imperfections in the Si mould. To apply a well-defined load, a motorized z-stage was used in combination with a force gauge. The size of the square pressure-sensitive pad was 64 mm^2. A small glass plate of equal size ('zero weight', 10 mg) was placed between the capacitor surface and force gauge tip, offering two benefits: (1) improved lamination between the two flexible film sheets and (2) increased area over which the force was applied, enabling measurement of very low pressures. Figure 2a shows the pressure response for two consecutive measurements (first run, filled symbols; second run, open symbols) of pressure sensitivity on three different PDMS film types: pyramidal, linear and unstructured (planar thin film). The pressure sensitivity S can be defined as the slope of the traces in Fig. 2a ($S = \delta(\Delta C/C_0)/\delta p = (1/C_0)^*\delta C/\delta p$, where p denotes the applied pressure, and C and C_0 denote the capacitances with and without applied pressure, respectively). The pressure sensitivity of the unstructured film (0.02 kPa^{-1}) was substantially lower than those of the structured films. In the <2 kPa pressure range, the sensitivity of the line-structured films was five times larger than that of the unstructured film (0.1 kPa^{-1}), and the pyramids showed a sensitivity of 0.55 kPa^{-1}, currently highest for a plastic thin-film pressure sensor. Both types of microstructured film show very little hysteresis (Fig. 2a, Supplementary Fig. S1) and can be reproducibly cycled thousands of times (Supplementary Fig. S2). The 6 × 6 μm^2 pyramid-structured PDMS films can reliably detect the placement or removal of an ultrasmall weight such as a bluebottle fly (weight: 20 mg) onto a small glass plate that covers the entire sensor area (Fig. 2c). This corresponds to a very small pressure of only 3 Pa. We are not aware of any flexible pressure sensor with such high sensitivity to the application of static pressure loads. The dramatic increase in sensitivity of the structured films over the unstructured films can be attributed to two main factors: (1) there is far less elastic resistance in the structured films because of the air voids in the PDMS film, and (2) when the structured films are compressed the displaced volume is air, which has a lower dielectric constant ($\varepsilon = 1.0$) than PDMS ($\varepsilon \sim 3.0$). Therefore, the increase in capacitance in the structured film arises from the reduction in the distance between the two electrode plates, and is enhanced further by the increase in effective dielectric constant. Hence, the pyramid-structured PDMS film in particular gave an almost 30-fold improvement in the pressure sensitivity compared with the unstructured film. There is a reduction in sensitivity at pressures > 2 kPa, which is most noticeable in the pyramid-structured films, where the sensitivity dropped to about $S \sim 0.15$ kPa^{-1}. In real-world applications this is desirable, because this progressive damping increases the range of detectable pressure to higher loads, at which high sensitivity is not required. The sensitivity decrease is attributed to the increasing elastic resistance

with increasing compression, dependent on the specific shape of the microstructure. These results indicate that both sensitivity and pressure range are tunable by modifying the shape of the PDMS structures. Films with higher sensitivity (pyramidal-like structures) can be imagined being used for sensor areas requiring both high sensitivity and resolution to static pressure, such as fingertips. In either regime, the base-signal-normalized sensitivity S of the pyramid-structure PDMS film compares very favourably with the sensitivity values achieved in previous reports: 0.05 kPa^{-1} (ref. 8); 0.008 kPa^{-1} (ref. 12); 0.005 kPa^{-1} (ref. 14); 5×10^{-4} kPa^{-1} (ref. 15); 0.02 kPa^{-1} (ref. 17); 0.001 kPa^{-1} (ref. 18); 10^{-4} kPa^{-1} (ref. 20).

The second main benefit of using structured PDMS films is illustrated by the sensor's response and relaxation times shown in Fig. 2b. As mentioned before, the visco-elastic behaviour in solid thin films of PDMS is problematic for pressure-sensor applications. Figure 2b shows the response and relaxation times of the structured and unstructured films (6 µm feature size) corresponding to the loading and unloading of the sensor. Although the response to an external load was immediate in both films (within experimental accuracy of the capacitance meter), the relaxation times were quite disparate, with structured films relaxing on the millisecond timescale, and unstructured films relaxing over times as long as 10 s. This lengthy response time of unstructured PDMS films severely limits their usefulness as pressure sensors. The structured PDMS films, however, exhibit relaxation times in the millisecond range, which is about 10^4 times and 10–100 times faster than those in refs 21 and 15, respectively. The curves shown in Fig. 2b were recorded with a load of 15 kPa, but the behaviour of the three types of devices was unchanged at much lower loads (see also Fig. 2c), with consistently poor relaxation times for the unstructured films ($\gg$1 s). It is also important to note that the microstructured PDMS films are thin ($<$10 µm) and consequently have a high baseline capacitance, which gives the sensors robustness to parasitic capacitances in the readout circuitry, and therefore a good signal-to-noise ratio. With foam-based capacitance sensors[15] the base capacitances are typically lower owing to the high thickness of the foam material, and are thus more susceptible to noise. The microstructured capacitance sensors also demonstrate excellent mechanical robustness to repeated mechanical stress (see Supplementary Figs S3 and S4).

Although there is a moderate dependence of the pressure response on the ambient temperature (Supplementary Fig. S2), the dependence is reversible, with a signal shift of 0.3 $kPa\,K^{-1}$ at 9 kPa applied pressure. This effect is most likely due to the thermal expansion of PDMS. However, the signal shift is significantly smaller than the values reported for the PRESSFET (ref. 9) (4.3 $kPa\,K^{-1}$) and polyvinylidene fluoride-based sensors[19] (64 $kPa\,K^{-1}$). A combination of temperature and pressure sensing, similar to that realized in ref. 1, can be used to correct for the signal shift.

Using the microstructured PDMS films, we fabricated prototype OFETs employing the highly pressure-sensitive PDMS film as the dielectric layer. The rationale for using the compressible films in OFET devices is the direct dependence of the electrical current in the transistor on the gate dielectric capacitance. Such pressure-sensitive OFETs can be arrayed in a low-impedance-output active-matrix design, reducing power consumption, as current only flows when the OFET is switched on. The layout of the pressure-sensitive OFET device is schematically shown in Fig. 3a. A thin and flat rubrene single crystal, grown using physical vapour transport[25,26], was laminated on top of bottom-contact gold electrodes on a highly n-doped silicon oxide wafer. These crystals typically exhibit a field-effect hole mobility on the order of 1 $cm^2\,V^{-1}\,s^{-1}$ (Supplementary Fig. S3). A single-crystal semiconductor was chosen because its structural perfection and low surface density of traps yield devices with very low threshold to transistor operation. Thin-film organic semiconductors with similar characteristics are also applicable here.

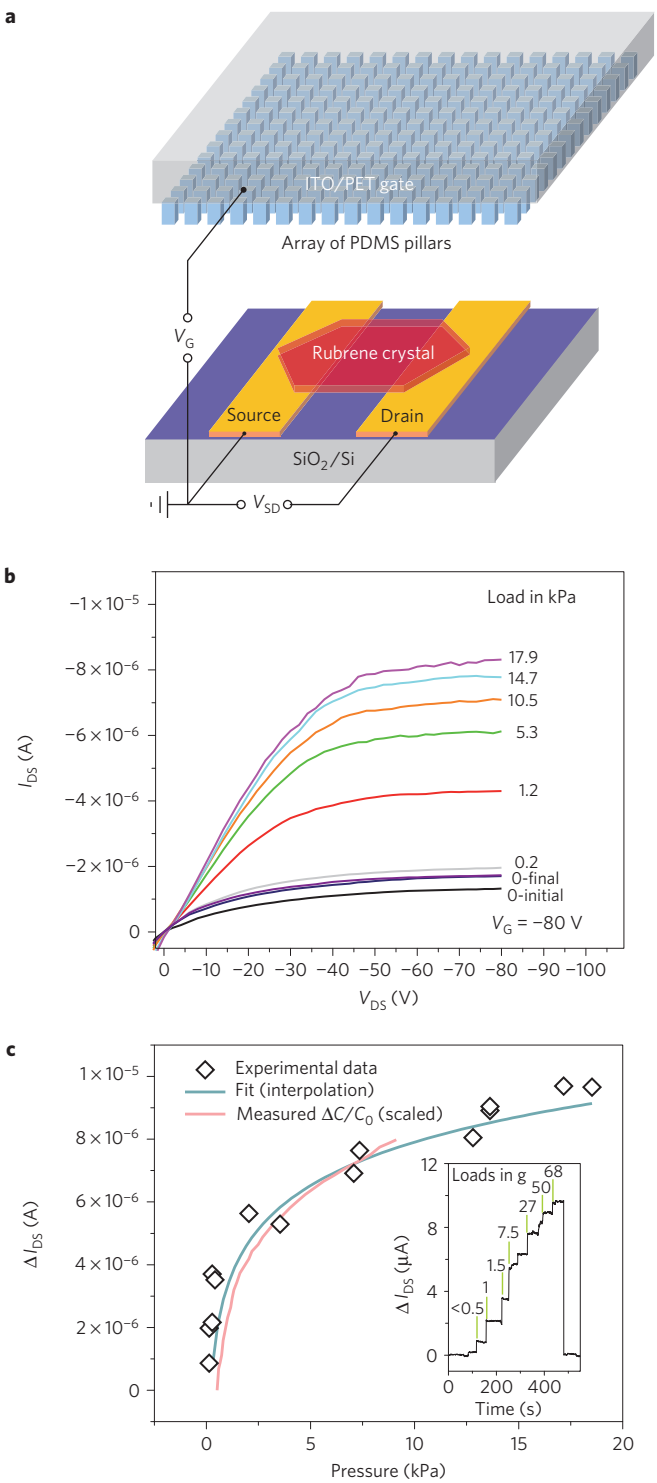

Figure 3 | Pressure response of an organic transistor with a microstructured PDMS dielectric layer. a, Layout of pressure-sensing organic single-crystal transistors, consisting of thin rubrene single crystals and structured PDMS dielectric films. **b**, Output curves ($I_{DS}(V_{DS})$) of a transistor-based sensor with different external pressures applied. The legend lists the applied loads in the order of the original loading cycle. **c**, The change in I_{DS}, ΔI_{DS} (diamond symbols), is proportional to the measured relative change in capacitance, $\Delta C/C_0$ (scaled data from Fig. 2a overlaid as red curve), as expected in the OFET saturation regime. The gate current remained more than two orders of magnitude below I_{DS}. The inset shows time-resolved measurements with excellent response and relaxation times.

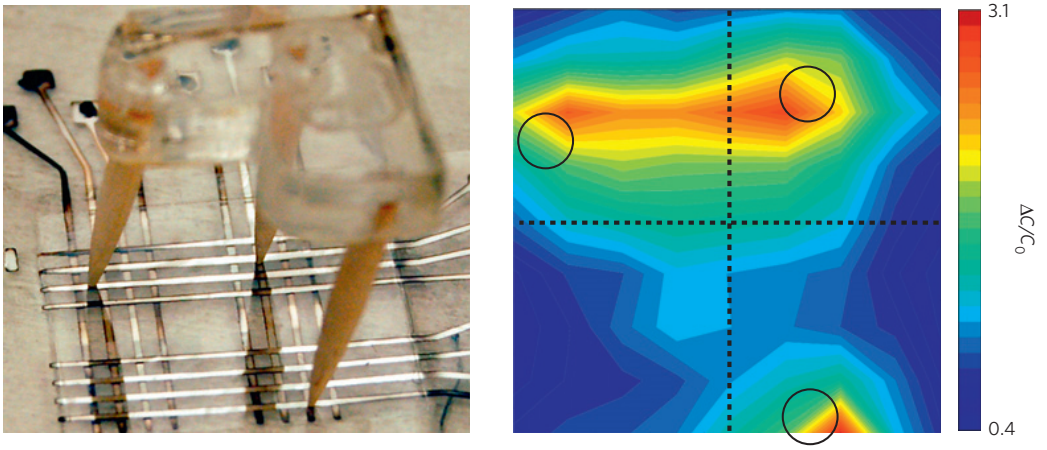

Figure 4 | Plastic and flexible pixel-type pressure-sensor arrays. These were built using a microstructured PDMS film sandwiched between electrode-containing PET sheets. The pressure response to the tripod is shown on the right.

A pyramid-structured PDMS film on flexible ITO/PET was then inverted and laminated to the crystal substrate to complete the transistor-based sensor, and the operation of the transistor was confirmed before pressure-sensor measurements were collected.

For the measurements with the flexible pressure-sensitive top-gate chip, the bottom gate was set to ground. Figure 3b shows a series of output curves as a function of external pressure, p. The current increased in discrete steps in response to successively greater loads. This increase can be attributed to compression of the dielectric layer (resulting in a reduction of the layer thickness), which simultaneously increases capacitance and the gate electric field at the dielectric–semiconductor interface. The inset of Fig. 3c shows the time-resolved response of the source–drain current $\Delta I_{DS}(p) = I_{DS}(p) - I_{DS0}$ in different loading and unloading experiments. Here, $I_{DS}(p)$ and I_{DS0} denote the source–drain current with and without application of an external pressure p, respectively. Different loading levels can be clearly distinguished, with excellent response and quick relaxation times.

In OFET devices, I_{DS} depends linearly on the dielectric capacitance. Accordingly, a nonlinear response in the source–drain current to the application of pressure, similar to the nonlinear pressure dependence of PDMS film capacitance (Fig. 2a), is expected, as $\Delta I_{DS}(p) = I_{DS}(p) - I_{DS0} = k(\Delta C/C_0)$, with k being a proportionality constant, dependent on device geometry, materials and the biases applied to the device terminals. Figure 3c compares the pressure response $\Delta I_{DS}(p)$ of the OFET device at fixed voltage with the capacitance response $\Delta C/C_0$ (see Fig. 2a). The ΔI_{DS} values are plotted as a function of the applied pressure p together with an interpolated curve (green) and the $\Delta C/C_0$ response from Fig. 2a, scaled to match the $\Delta I_{DS}(p)$ curve at a pressure of 7 kPa (red). The two curves match well, demonstrating that the change of the structured PDMS film capacitance is indeed linearly transformed into a change in the transistor's source–drain current. In the time-resolved measurements, the OFET devices exhibit similarly rapid millisecond-regime response and relaxation times to the capacitive sensors (Fig. 3c inset and Supplementary Fig. S7). The sensors can operate stably at bias voltages as low as −20 V (Supplementary Fig. S5). In future, the operation voltage can be further lowered substantially by a reduction in the dielectric thickness[6] and/or using materials with higher dielectric constant.

We have also produced a proof-of-concept capacitive matrix-type pressure sensor that is flexible and, apart from the metal electrodes, an 'all-plastic' device (Fig. 4). The device was fabricated by sandwiching the microstructured PDMS film between two PET substrates (25 μm thick), each of which contained a set of eight vacuum-deposited aluminium metal lines (150 μm wide) that served as address and data lines. This 8 × 8 pixel pressure sensor-pad was partitioned into four quadrants each using a 64 mm^2 area of microstructured PDMS film (this area limitation is arbitrary and strictly due to the layout of the Si mould). The right panel in Fig. 4 shows the response of the device to the placement of a small weight on a tripod (3.78 g), where a darker colour corresponds to a higher capacitance. The areas of high capacitance and thus greater compression corresponded well to the locations of the three legs (indicated by the black circles). The resolution of the present device is limited by the shadow-mask-defined electrodes and the elastic properties of the two plastic substrates. To decrease the spillover of the signal from an addressed pixel into the neighbouring sensor areas, the lateral size of the indention in the top terminal caused by local pressure application needs to be as small as possible. This can be achieved by using stretchable materials in place of PET. The matrix pressure sensor also demonstrates the possibility for use in multitouch devices that enable pressure information to be collected at multiple points.

High-definition structuring of thin elastomeric films significantly alters the mechanical properties of these films beneficially, providing a greater design space for fast, flexible and responsive pressure sensors. Both passive capacitor devices and active OFET sensor devices employing these microstructured elastomeric dielectric films have been demonstrated, exhibiting unprecedented pressure sensitivities. The fast response times in these sensors allows for a rapid collection of pressure information on both flat and curvilinear surfaces, which will potentially enable the development of highly intuitive human–computer user interfaces. The very high sensitivity, large workable pressure range and simple fabrication of these pressure sensors, based on a flexible, bio-compatible microstructured rubber dielectric material, make them promising candidates for electronic-skin applications.

Methods

The moulds—made from ⟨100⟩ wafers with a 300 nm thermally grown oxide—were patterned using photolithography, and the oxide was used as a mask for the potassium hydroxide etch. The oxide was stripped using buffered hydrofluoric acid, followed by vapour deposition of tridecafluoro-1,1,2,2,-tetrahydrooctyl trichlorosilane (Gelest) to facilitate release of the mould. A 5:1 mixture of PDMS elastomer (Sylgard 184, Dow Corning) to cross-linker was prepared and diluted with hexane (10:1 hexane to PDMS mixture) and stirred for at least 30 min. 100 μl of the diluted solution was then transferred onto the mould and degassed. A 150-μm-thick PET film with conductive ITO was then ultraviolet-ozone-treated for 20 min and placed on top of the degassed PDMS film in vacuum. The entire stack was then clamped with a pressure of >100 MPa at a temperature of 70 °C for at least 4 h. Moulded PDMS films on PET and silicon substrates were coated with a thin layer of gold (8–10 nm) before imaging with an FEI XL30 Sirion SEM. The accelerating voltage was 5 kV.

Capacitance measurements were taken using the Agilent E4980A Precision *LCR* meter. Capacitances were measured at 1 kHz frequency with a 1 V a.c. signal. A mechanized *z*-axis stage (Newmark Systems, 0.1 μm resolution) and force gauge (Dillion GL model, 0.5 g resolution) were used to apply loads to the sensor pads on a custom-built probe station, all interfaced through a computer.

Single rubrene crystals were grown by the physical vapour transport method (see refs 26,27) at atmospheric pressure in high-purity argon at approximately 80 ccm. Rubrene (obtained from Aldrich) was first purified through three-zone vacuum sublimation. Crystals varied in thickness from hundreds of nanometres to several micrometres. Only very thin, flexible crystals were chosen for this experiment.

Transistor measurements were made in bottom-contact, top-gate geometry. Bottom-contact electrode arrays were fabricated by thermal evaporation of a Cr adhesion layer (1.5 nm) and Au (30 nm) through a shadow mask onto highly n-doped SiO_2 wafers with a 300 nm thermal oxide. The electrical characterization of the transistor devices was carried out in ambient conditions using a Keithley 4200SCS semiconductor parameter analyser, and loads were applied with a force gauge (see above).

Matrix-type capacitance pressure sensors were prepared from a 25 μm PET film (3 M) by cleaning through sonication in acetone and isopropanol before evaporation of 150-nm-thick aluminium lines through a shadow mask. A moulding procedure similar to the one described above was followed to put down the microstructured PDMS film on top of the metal lines.

Received 15 March 2010; accepted 16 July 2010; published online 12 September 2010

References

1. Someya, T. *et al.* Conformable, flexible, large-area networks of pressure and thermal sensors with organic transistor active matrixes. *Proc. Natl Acad. Sci.* **102,** 12321–12325 (2005).
2. Sekitani, T. *et al.* A rubberlike stretchable active matrix using elastic conductors. *Science* **321,** 1468–1472 (2008).
3. Wagner, S. *et al.* Electronic skin: Architecture and components. *Physica E* **25,** 326–334 (2004).
4. Sun, Y., Choi, W. M., Jiang, H., Huang, Y. Y. & Rogers, J. A. Controlled buckling of semiconductor nanoribbons for stretchable electronics. *Nature Nanotech.* **1,** 201–207 (2006).
5. Dellon, E. S., Mourey, R. & Dellon, A. L. Human pressure perception values for constant and moving one- and two-point discrimination. *J. Plast. Reconstr. Surg.* **90,** 112–117 (1992).
6. Bao, Z. & Locklin, J. *Organic Field-Effect Transistors* (CRC Press, 2007).
7. Roberts, M. E. *et al.* Water-stable organic transistors and their application in chemical and biological sensors. *Proc. Natl Acad. Sci.* **105,** 12134–12139 (2008).
8. Someya, T. *et al.* A large-area, flexible pressure sensor matrix with organic field-effect transistors for artificial skin applications. *Proc. Natl Acad. Sci.* **101,** 9966–9970 (2004).
9. Voorthuyzen, J. A., Bergveld, P. & Sprenkels, A. J. Semiconductor-based electret sensors for sound and pressure. *IEEE Trans. Electr. Insul.* **24,** 267–276 (1989).
10. Olthuis, W. Chemical and physical FET-based sensors or variations on an equation. *Sens. Actuat. B* **105,** 96–103 (2005).
11. Hussain, M., Choa, Y-H. & Niihara, K. Conductive rubber materials for pressure sensors. *J. Mater. Sci. Lett.* **20,** 525–527 (2001).
12. Shimojo, M., Namiki, A., Ishikawa, M., Makino, R. & Mabuchi, K. A tactile sensor sheet using pressure conductive rubber with electrical-wires stitched method. *IEEE Sensors J.* **4,** 589–596 (2004).
13. Engel, J., Chen, J., Chen, N., Pandya, S. & Liu, C. *19th International Conference on MEMS, Istanbul, Turkey* (IEEE, 2006).
14. Lee, H-K., Chang, S-I. & Yoon, E. A flexible polymer tactile sensor: Fabrication and modular expandability for large area deployment. *J. Microelectromech. Syst.* **15,** 1681–1686 (2006).
15. Metzger, C. *et al.* Flexible-foam-based capacitive sensor arrays for object detection at low cost. *Appl. Phys. Lett.* **92,** 013506 (2008).
16. Lee, I. & Sung, H. J. Development of an array of pressure sensors with PVDF film. *Exp. Fluids* **26,** 27–35 (1999).
17. Shirinov, A. V. & Schomburg, W. K. Pressure sensor from a PVDF film. *Sens. Actuat. A* **142,** 48–55 (2008).
18. Graz, I. *et al.* Flexible ferroelectret field-effect transistor for large-area sensor skins and microphones. *Appl. Phys. Lett.* **89,** 073501 (2006).
19. Graz, I. *et al.* Flexible active-matrix cells with selectively poled bifunctional polymer–ceramic nanocomposite for pressure and temperature sensing skin. *J. Appl. Phys.* **106,** 034503 (2009).
20. Darlinski, G. *et al.* Mechanical force sensors using organic thin-film transistors. *J. Appl. Phys.* **97,** 093708 (2005).
21. Manunza, I., Sulis, A. & Bonfiglio, A. Pressure sensing by flexible, organic, field effect transistors. *Appl. Phys. Lett.* **89,** 143502 (2006).
22. Chan, Y., Mi, Y., Trau, D., Huang, P. & Chen, E. Micromolding of PDMS scaffolds and microwells for tissue culture and cell patterning: A new method of microfabrication by the self-assembled micropatterns of diblock copolymer micelles. *Polymer* **47,** 5124–5130 (2006).
23. Balaban, N. Q. *et al.* Force and focal adhesion assembly: A close relationship studied using elastic micropatterned substrates. *Nature Cell Biol.* **3,** 466–472 (2001).
24. Reese, C., Chung, W-J., Ling, M-M., Roberts, M. E. & Bao, Z. High-performance microscale single-crystal transistors by lithography on an elastomer dielectric. *Appl. Phys. Lett.* **89,** 202108 (2006).
25. Sundar, V. C. *et al.* Elastomeric transistor stamps: Reversible probing of charge transport in organic crystals. *Science* **303,** 1644–1646 (2004).
26. Kloc, Ch., Simpkins, P. G., Siegrist, T. & Laudise, R. A. Physical vapour growth of centimetre-sized crystals of alpha-hexathiophene. *J. Cryst. Growth* **182,** 416–427 (1997).
27. Reese, C. & Bao, Z. Organic single-crystal field-effect transistors. *Mater. Today* **10,** 20–27 (2007).

Acknowledgements

The authors thank J. Locklin for discussions. We thank N. Sutardja and J. Opatkiewicz for help during the development of the microstructuring technology and the first sensor prototypes. This project was partially funded by NSF ECCS 0730710 and MURI Office of Naval Research (N000140810654). We thank the Center for Polymer Interface Macromolecular Assemblies (CPIMA) for the use of shared facilities. We also acknowledge the use of the Stanford Nanocharacterization Laboratory and the Stanford Nanofabrication Facility, partially supported by the National Science Foundation through the National Nanotechnology Infrastructure Network. Part of this work was done at the Stanford Synchrotron Radiation Laboratory (SSRL), operated by the Department of Energy. S.C.B.M. acknowledges postdoctoral fellowship support by the Deutsche Forschungsgemeinschaft (DFG) grant MA ∼ 3342/1-1. B.C-K.T. acknowledges support from a National Science Scholarship from the Agency for Science, Technology and Research (A∗STAR), Singapore. R.M.S. acknowledges support from a National Science Foundation Graduate Fellowship. Z.B. acknowledges support from a Sloan Research Fellowship.

Author contributions

Z.B. and S.C.B.M. conceptualized and directed the research project. S.C.B.M. developed the first working sensor prototypes. B.C-K.T. developed large portions of the experimental set-ups. S.C.B.M and B.C-K.T. discussed and carried out the majority of the experiments. B.C-K.T. and C.V.H-H.C designed and fabricated the matrix sensor. B.C-K.T. carried out the temperature drift and loading/unloading stability experiments. R.M.S. took the SEM data. S.B. helped with some experiments. R.M.S., B.C-K.T. and B.V.O.M fabricated the Si moulds. B.V.O.M. fabricated the photolithographic mask. A.N.S. and B.C-K.T carried out most of the bending-stability experiments. C.R. and B.C-K.T. grew the rubrene crystals. S.C.B.M. wrote the first draft of the manuscript. All authors discussed the results and commented on the manuscript.

Additional information

The authors declare competing financial interests: details accompany the paper at www.nature.com/naturematerials. Supplementary information accompanies this paper on www.nature.com/naturematerials. Reprints and permissions information is available online at http://npg.nature.com/reprintsandpermissions. Correspondence and requests for materials should be addressed to Z.B.